IEEE Access
Multidisciplinary ⁝ Rapid Review ⁝ Open Access Journal

Received January 4, 2018, accepted February 2, 2018, date of publication February 22, 2018, date of current version March 15, 2018.

Digital Object Identifier 10.1109/ACCESS.2018.2808170

Adaptive Strong Tracking Square-Root Cubature Kalman Filter for Maneuvering Aircraft Tracking

HAOWEI ZHANG[1], JUNWEI XIE[1], JIAANG GE[1], WENLONG LU[2], AND BINFENG ZONG[3]
[1]Air and missile Defense College Air Force Engineering University, Xi'an 710051, China
[2]Unit 94225, Rizhao 276000, China
[3]Unit 94710, Wuxi 214000, China

Corresponding author: Haowei Zhang (zhw_xhzf@163.com)

This work was supported by the National Youth Foundation of China under Grant 61503408 and Grant 61601504.

ABSTRACT A novel strong tracking square-root cubature Kalman filter (SCKF) based on the adaptive current statistical (CS) model is proposed aiming at the maneuvering aircraft tracking problem. The Jerk input estimation is introduced on the basis of the modified input estimation algorithm in order to make the connection with the state process noise and the state error covariance matrix. Thus, the online-adaptive adjustment of the CS model is achieved. Additionally, the introduced position of the fading factor is re-deduced and a novel calculation method is designed in order to overcome the invalidity problem of the traditional fading factor. Two simulation scenarios are conducted to verify the effectiveness of the proposed algorithm. The simulation results show that the proposed algorithm possesses better adaptability and tracking precision than the two state-of-the-art single model filters. Moreover, the proposed algorithm decreases the runtime by 40% while maintaining the comparable performance compared with the interacting-multiple-model SCKF.

INDEX TERMS Aircraft tracking; current statistical (CS) model, square-root cubature Kalman filter (SCKF), modified input estimation (MIE), fading factor.

I. INTRODUCTION

Model errors are inevitable in the maneuvering aircraft tracking problem, whose reasons are the model mismatch, the unknown disturbance and the nonlinear and non-Gaussian property of the measurement. Therefore, the elimination of model errors may be performed by the following means. One is to improve the accuracy and the adaptive adjustment capability of the structured model. Another is to improve the precision of the filtering algorithm. The modeling for highly maneuvering aircraft can be roughly divided into single model and multiple categories. Though the later algorithm tries its best to utilize multiple models to match the maneuvering process, models can't cover all motion states. In addition, the increase in the number of model naturally leads to a decrease in the real-time property of the algorithm. As to the single model algorithm, references [1]–[3] propose the Singer model [1], current statistical (CS) model [2], and Jerk model [3] successively, where the CS model has the better ability to describe the aircraft maneuvering character compared with others. However, the CS model has some inherent problems such as the need of presetting prior parameters and the lack of adaptive adjustment capability. Though references [4]–[6] put forward many modified CS models, they all concentrate on mending some parameters in the CS model and don't touch its innate character. Additionally, the aircraft data is measured in polar coordinates whereas the aircraft motion model is established in the Cartesian coordinate system. Thus, a nonlinear transformation is required. Recently, nonlinear estimation methods - Gaussian approximation filters [7]–[13] based on the sample point, have been involving in intensive research. Typical ones are the unscented Kalman filter (UKF) [7], [8], the Gauss-Hermite quadrature filter (GHQF) [9], [10] and the cubature Kalman filter (CKF) [11]–[13]. Due to the avoidance of calculating Jacobian matrix and the utilization of nonlinear model of the system instead of linearization, they have great advantages over the extended Kalman filter (EKF) [13]. Especially, the CKF shows merits of low computational complexity and strong robustness among them and thus is applied in various state estimation problems [16]–[18]. Moreover, the square-root CKF (SCKF) introduces the matrix triangular factorization based on the CKF and avoids the recursive square-root operation to the state error covariance matrix, improving the numerical stability and accuracy further. However, the performance of the nonlinear filters will be greatly influenced when faced with the inaccurate model or bad measurement caused by the aircraft maneuver. In order to improve the tracking stability on the abrupt change, references [19]–[25] introduce the fading factor in the state error covariance matrix and structure the strong tracking (ST) nonlinear filter. However, the fading factor in [19]–[25] has two problems. The first is the arbitrariness of the introduced position, which is due to a lack of mathematical deduction to the simultaneous satisfaction of the orthogonality principle of residual error sequences and of the least mean-square error of the output estimation. The second one is that they all adopt the form of the ratio between the identification value of sum of diagonal elements in the measurement residual error covariance matrix and the theoretical output value from the filter, bringing about two problems in the radar measurement coordinate. One is that the sum of diagonal elements in the residual error covariance matrix is meaningless because different dimensional residual errors have different meanings. The other is that the angular residual error is greatly smaller than the other dimensions. When the abrupt change mainly occurs in the angle dimension, the small change of the angular residual error has little effect on the change of the fading factor and thus the fading factor will be invalid.

An adaptive CS model is proposed and the SCKF is adopted for the state estimation in this paper aiming at the issues above. Additionally, the introduced position of the fading factor is relocated and a novel calculation formula for the fading factor is put forward for the purpose of improving the algorithm performance on tracking maneuvering aircrafts. The main contributions of this paper are as follows.

The first is that an adaptive CS model is proposed. The Taylor's series expansion of the acceleration mean in the CS model and the modified input estimation (MIE) [26] algorithm are combined to introduce the Jerk input estimation and to modify the state equation and the adjustment method of maneuvering acceleration covariance matrix in the CS model. Thereby, the process noise and the state error covariance matrix output from the filter are connected and the adaptive tracking to the aircraft is realized.

The second one is that the sufficient condition of the ST-SCKF is re-deduced from the orthogonality principle and the effective position of the fading factor is relocated.

The third one is that a new calculation method is put forward for the fading factor. The maximum ratio between the vector structured by diagonal elements in the measurement residual error covariance matrix and the vector structured by diagonal elements in the theoretical output value from the filter is utilized for the calculation of the fading factor. Thereby, the invalidity problem of traditional fading factors can be avoided.

Last but not the least, two simulation scenarios conducted show that the proposed algorithm is able to accurately track highly maneuvering motion and weak maneuvering motion at the condition of lacking prior knowledge. The performance of the proposed algorithm is better than the multiple-fading-factor SCKF [24] based on the CS model and the SCKF-STF [25] based on the modified CS model [6]. Moreover, the proposed algorithm decreases the runtime by 40% while maintaining the commensurate performance compared with the interacting-multiple-model SCKF (IMM-SCKF).

II. ANALYSIS ON THE CS MODEL

The discrete state equation of the CS model and the nonlinear measurement equation are shown in Eq. (1) and Eq. (2) respectively.

$$\boldsymbol{X}_{k+1} = \boldsymbol{F}_k\boldsymbol{X}_k + \boldsymbol{U}_k\bar{\boldsymbol{a}}_k + \boldsymbol{W}_k = f(\boldsymbol{X}_k) + \boldsymbol{W}_k \tag{1}$$

$$\boldsymbol{Z}_{k+1} = h(\boldsymbol{X}_{k+1}) + \boldsymbol{V}_{k+1} \tag{2}$$

where $\boldsymbol{F}_k$ is the state transition matrix. $\boldsymbol{U}_k$ is the acceleration input matrix. $\bar{\boldsymbol{a}}_k$ is the input acceleration mean. $\boldsymbol{Z}_{k+1}$ is the measurement matrix. $h(.)$ is the nonlinear transformation function. $\boldsymbol{W}_k \sim N(\boldsymbol{0}, \boldsymbol{Q}_k)$, the process noise. $\boldsymbol{V}_{k+1} \sim N(\boldsymbol{0}, \boldsymbol{R}_{k+1})$, the measurement noise. $\boldsymbol{W}_k$ and $\boldsymbol{V}_{k+1}$ are mutually independent. $\boldsymbol{Q}_k = 2\alpha\sigma_a^2\boldsymbol{q}_{\text{cs}}$. α is the maneuvering frequency. Specific forms of $\boldsymbol{F}_k$, $\boldsymbol{U}_k$ and $\boldsymbol{q}_{\text{cs}}$ can be found in [2], and [4]–[6]. σ_a^2, the variance of maneuvering acceleration, complies with the mended Rayleigh distribution:

$$\sigma_a^2 = \begin{cases} \dfrac{4-\pi}{\pi}(a_{\max} - \bar{a}_{k+1})^2 & \bar{a}_{k+1} \geq 0 \\ \dfrac{4-\pi}{\pi}(a_{\max} + \bar{a}_{k+1})^2 & \bar{a}_{k+1} < 0 \end{cases} \tag{3}$$

However, $\bar{a}_{k+1}$ is inaccessible. Thus, the following approximation is contained in the CS model [27]:

$$\bar{a}_{k+1}E[a_{k+1}|\boldsymbol{Z}^k] \approx E[a_k|\boldsymbol{Z}^k] \triangleq \hat{a}_k \tag{4}$$

where $\boldsymbol{Z}^k$ is the set of measurement till to time k. $\hat{a}_k$ is the acceleration estimation in time k. Thus, Eq. (3) indeed is:

$$\sigma_{a,k}^2 = \begin{cases} \dfrac{4-\pi}{\pi}\left(a_{\max} - \hat{a}_k\right)^2 & \hat{a}_k \geq 0 \\ \dfrac{4-\pi}{\pi}\left(a_{-\max} + \hat{a}_k\right)^2 & \hat{a}_k < 0 \end{cases} \tag{5}$$

Eq. (5) and $\boldsymbol{Q}_k = 2\alpha\sigma_a^2\boldsymbol{q}_{\text{cs}}$ reveal that the tracking performance of the CS model is dependent on two preset parameters: the maximum acceleration and the maneuvering frequency. If $a_{\pm\max}$ and α cover large scope, the tracking precision on the steady state and the weak maneuver will be greatly influenced. However, the real values will easily exceed the threshold if they are preset as low values, bringing about deteriorated tracking precision on maneuver state. Therefore, the CS model should be modified.

III. ADAPTIVE CS MODEL

According to Taylor's series expansion, the acceleration can be expressed as follows.

$$a(t) = a(t_0) + \frac{1}{1!}a^{(1)}(t_0)(t-t_0) + \frac{1}{2!}a^{(2)}(t_0)(t-t_0)^2 + \cdots + \frac{1}{n!}a^{(n)}(t_0)(t-t_0)^n \tag{6}$$

where $a^{(1)}(t_0)$ is the Jerk value in time t_0. $a^{(n)}(t_0)$ is n order derivative of $a(t)$ in t_0. Let $t_0 = kT$ and $t = (k+1)T$, where T is the sample interval, and Eq. (6) can be expressed as:

$$a_{k+1} = a_k + Ta_k^{(1)} + \frac{T^2}{2!}a_k^{(2)} + \frac{T^3}{3!}a_k^{(3)} + \cdots + \frac{T^n}{n!}a_k^{(n)} \quad (7)$$

Eq. (7) show that $a_{\pm\max}$ in time $(k+1)T$ is able to be deduced by the acceleration, Jerk and higher order derivatives in time kT. Therefore, Eq. (4) can be rewritten as:

$$\begin{aligned}\bar{a}_{k+1}&E[a_{k+1}|\mathbf{Z}^k] \\ &= E[a_k|\mathbf{Z}^k] + E[a_k^{(1)}|\mathbf{Z}^k]T \\ &\quad + E[a_k^{(2)}|\mathbf{Z}^k]\frac{T^2}{2!} + \cdots + E[a_k^{(n)}|\mathbf{Z}^k]\frac{T^n}{n!} \\ &= \hat{a}_k + T\hat{a}_k^{(1)} + \frac{T^2}{2!}\hat{a}_k^{(2)} + \frac{T^3}{3!}\hat{a}_k^{(3)} + \cdots + \frac{T^n}{n!}\hat{a}_k^{(n)} \quad (8)\end{aligned}$$

Eq. (3) can be rewritten as:

$$\sigma_{a,k}^2 = \frac{4-\pi}{\pi} \times \left(\tilde{a}_k + T\tilde{a}_k^{(1)} + \frac{T^2}{2!}\tilde{a}_k^{(2)} + \frac{T^3}{3!}\tilde{a}_k^{(3)} + \cdots + \frac{T^n}{n!}\tilde{a}_k^{(n)}\right)^2 \quad (9)$$

where $\tilde{a}_k^{(n)}$ is the estimation error of $a_k^{(n)}$. Eq. (9) indicates that the acceleration and the measurement variance are able to be adaptively adjusted in the CS model on the condition that the acceleration, the Jerk and the higher order derivatives in time kT are accessible. However, the higher order derivatives in time kT can't be obtained due to the dimension limitation. Therefore, the following two approximations are introduced into Eq. (8) and Eq. (9).

(1) The maximum acceleration $a_{\pm\max}$ in time $(k+1)T$ can be deduced by the real acceleration a_k and the Jerk mean $\bar{a}_k^{(1)}$ in time kT:

$$a_{\pm\max} = a_{k+1} \approx a_k + T\bar{a}_k^{(1)} \quad (10)$$

(2) The acceleration mean $\bar{a}_{k+1}$ in time $(k+1)T$ can be deduced by the estimation value of acceleration $\hat{a}_k$ and the mean estimation value of Jerk $\hat{\bar{a}}_k^{(1)}$ in time kT:

$$\bar{a}_{k+1} \approx \hat{a}_k + T\hat{\bar{a}}_k^{(1)} \quad (11)$$

Due to the unknown of $\hat{\bar{a}}_k^{(1)}$, the idea of MIE [26] is introduced to augment it in the state vector and the recursive least square estimation method is utilized. The equation of $\bar{\boldsymbol{a}}_{k+1}^{(1)} = \bar{\boldsymbol{a}}_k^{(1)}$ is supplemented with Eq. (1) to deduce the state equation of the adaptive CS model:

$$\begin{bmatrix}\boldsymbol{X}_{k+1} \\ \bar{\boldsymbol{a}}_{k+1}^{(1)}\end{bmatrix} = \begin{bmatrix}\boldsymbol{F}_{\mathrm{ACS}} & \boldsymbol{U}_{\mathrm{ACS}} \\ \boldsymbol{0} & \boldsymbol{I}\end{bmatrix}\begin{bmatrix}\boldsymbol{X}_k \\ \bar{\boldsymbol{a}}_k^{(1)}\end{bmatrix} + \begin{bmatrix}\boldsymbol{W}_k \\ \boldsymbol{0}\end{bmatrix} \quad (12)$$

where

$$\boldsymbol{F}_{\mathrm{ACS}} = \begin{bmatrix}1 & T & T^2/2 \\ 0 & 1 & T \\ 0 & 0 & 1\end{bmatrix}$$

and

$$\boldsymbol{U}_{\mathrm{ACS}} = \begin{bmatrix}T^3/6 - (2 - 2\alpha T + \alpha^2T^2 - 2e^{-\alpha T})/2\alpha^3 \\ T^2/2 - (e^{-\alpha T} - 1 + \alpha T)/\alpha^2 \\ T - (1 - e^{-\alpha T})/\alpha\end{bmatrix}.$$

Additionally, Eq. (9) is rewritten as follows based on approximations of Eq. (10) and Eq. (11).

$$\sigma_{a,k}^2 = \frac{4-\pi}{\pi}\left(\tilde{a}_k + T\tilde{\bar{a}}_k^{(1)}\right)^2 \quad (13)$$

where $\tilde{\bar{a}}_k^{(1)}$ is the estimation error of Jerk. Considering the occupied ratio of the Jerk mean in the adaptive CS model, the variance expectation of acceleration and the Jerk mean are utilized to approximate Eq. (13):

$$\begin{aligned}\sigma_{a,k}^2 &= \frac{4-\pi}{\pi}\left\{E[\tilde{a}_k\tilde{a}_k^{\mathrm{T}}] + 2TE[\tilde{\bar{a}}_k^{(1)}(\tilde{\bar{a}}_k^{(1)})^T] + T^2E[\tilde{a}_k(\tilde{\bar{a}}_k^{(1)})^T]\right\} \\ &= \frac{4-\pi}{\pi}\left\{\boldsymbol{P}_k(\ddot{x},\ddot{x}) + 2T\boldsymbol{P}_k(\bar{x},\bar{x}) + T^2\boldsymbol{P}_k(\ddot{x},\bar{x})\right\} \quad (14)\end{aligned}$$

where $\boldsymbol{P}_k(.,.)$ is the corresponding elements in the output state covariance matrix of the filter.

Above all, the adaptive CS model is transformed into the standard filtering model, and the process noise is connected with the state covariance output from the filter by the modeling of the maximum acceleration and the mean value of acceleration. Thereby, the adaptive tracking to the aircraft is able to be realized.

IV. SCKF WITH MODIFIED FADING FACTOR

A. SCKF

CKF, essentially a Gaussian approximation filter, transforms the nonlinear filtering problem with Gauss distribution into the quadrature calculation problem. SCKF introduces the square-root of state error covariance matrix on the basis of CKF in order to ensure the positive definiteness and to further improve the filtering stability and precision.

Before describing the procedure of the SCKF, the operation symbol Tria(.) is defined as follows. $\boldsymbol{R}$ is the upper triangular matrix obtained from the QR decomposition on matrix $\boldsymbol{A}^T$, so the QR decomposition operation to $\boldsymbol{A}$ can be expressed as $\boldsymbol{S} = Tria(\boldsymbol{A}) = \boldsymbol{R}^T$, where $\boldsymbol{S}$ is the lower triangular matrix. The procedure of SCKF [11], [12] is able to be described as follows.

Step 1: Time update

Assume that state error covariance is $P_{k|k}$ in time kT, then

Step 1.1: Factorize

$$\boldsymbol{P}_{k|k} = \boldsymbol{S}_{k|k}(\boldsymbol{S}_{k|k})^T \quad (15)$$

Step 1.2: Evaluate the cubature points and the propagated cubature points

$$\boldsymbol{X}_{k|k}^i = \hat{\boldsymbol{X}}_{k|k} + \boldsymbol{S}_{k|k}\boldsymbol{\xi}_i, \quad i = 1, 2 \ldots m \quad (16)$$

$$\boldsymbol{X}_{k+1|k}^{i*} = f(\boldsymbol{X}_{k|k}^i) \quad (17)$$

where $\boldsymbol{X}_{k|k}^i$ and $\boldsymbol{X}_{k+1|k}^{i*}$ are the cubature point and the propagated cubature point respectively. m is the total number of cubature points, n is the dimensional number of the state vector $\boldsymbol{X}$, which satisfies $m = 2n$. $\xi_i = (\mathrm{m}/2)^{1/2}[\mathbf{1}]$, $[\mathbf{1}]$ is the full permutation and reverse of n dimensional unit vector:

$$[\mathbf{1}] = \left\{ \begin{pmatrix} 1 \\ 0 \\ \cdots \\ 0 \end{pmatrix}, \begin{pmatrix} 0 \\ 1 \\ \cdots \\ 0 \end{pmatrix}, \ldots, \begin{pmatrix} 0 \\ 0 \\ \cdots \\ 1 \end{pmatrix}, \begin{pmatrix} -1 \\ 0 \\ \cdots \\ 0 \end{pmatrix}, \begin{pmatrix} 0 \\ -1 \\ \cdots \\ 0 \end{pmatrix}, \ldots, \begin{pmatrix} 0 \\ 0 \\ \cdots \\ -1 \end{pmatrix} \right\} \tag{18}$$

Step 1.3: Estimate the predicted state and the square-root factor of the predicted error covariance.

$$\hat{\boldsymbol{X}}_{k+1|k} = \frac{1}{m}\sum_{i=1}^{m} \boldsymbol{X}_{k+1|k}^{i*} \tag{19}$$

$$\boldsymbol{S}_{k+1|k} = \mathrm{Tria}([\boldsymbol{X}_{k+1|k}^{*}, \mathrm{Chol}(\boldsymbol{Q}_k)]) \tag{20}$$

where the weighted, centered matrix

$$\boldsymbol{X}_{k+1|k}^{*} = \frac{1}{\sqrt{m}}\left[\boldsymbol{X}_{k+1|k}^{1*} - \hat{\boldsymbol{X}}_{k+1|k}, \boldsymbol{X}_{k+1|k}^{2*} - \hat{\boldsymbol{X}}_{k+1|k}, \ldots, \boldsymbol{X}_{k+1|k}^{m*} - \hat{\boldsymbol{X}}_{k+1|k}\right] \tag{21}$$

Step 2: Measurement update

Step 2.1: Evaluate the cubature points and the propagated cubature points

$$\boldsymbol{X}_{k+1|k}^{i} = \hat{\boldsymbol{X}}_{k+1|k} + \boldsymbol{S}_{k+1|k}\boldsymbol{\xi}_i \tag{22}$$

$$\boldsymbol{Z}_{k+1|k}^{i} = h(\boldsymbol{X}_{k+1|k}^{i}) \tag{23}$$

Step 2.2: Estimate the predicted measurement

$$\hat{\boldsymbol{Z}}_{k+1|k} = \frac{1}{m}\sum_{i=1}^{m} \boldsymbol{Z}_{k+1|k}^{i} \tag{24}$$

Step 2.3: Estimate the square-root of the residual error (innovation) covariance matrix

$$\boldsymbol{S}_{k+1|k}^{ZZ} = \mathrm{Tria}([\boldsymbol{Z}_{k+1|k}, \mathrm{Chol}(\boldsymbol{R}_{k+1})]) \tag{25}$$

where the weighted, centered matrix

$$\boldsymbol{Z}_{k+1|k} = \frac{1}{\sqrt{m}}\left[\boldsymbol{Z}_{k+1|k}^{1} - \hat{\boldsymbol{Z}}_{k+1|k}, \boldsymbol{Z}_{k+1|k}^{2} - \hat{\boldsymbol{Z}}_{k+1|k}, \ldots, \boldsymbol{Z}_{k+1|k}^{m} - \hat{\boldsymbol{Z}}_{k+1|k}\right] \tag{26}$$

Step 2.4: Calculate the residual error covariance matrix

$$\boldsymbol{P}_{k+1|k}^{ZZ} = \boldsymbol{S}_{k+1|k}^{ZZ}(\boldsymbol{S}_{k+1|k}^{ZZ})^T \tag{27}$$

Step 2.5: Estimate the cross-covariance matrix between the state prediction error vector and the residual error vector

$$\boldsymbol{P}_{k+1|k}^{XZ} = \boldsymbol{X}_{k+1|k}(\boldsymbol{Z}_{k+1|k})^T \tag{28}$$

where the weighted, centered matrix

$$\boldsymbol{X}_{k+1|k} = \frac{1}{\sqrt{m}}\left[\boldsymbol{X}_{k+1|k}^{1} - \hat{\boldsymbol{X}}_{k+1|k}, \boldsymbol{X}_{k+1|k}^{2} - \hat{\boldsymbol{X}}_{k+1|k}, \ldots, \boldsymbol{X}_{k+1|k}^{m} - \hat{\boldsymbol{X}}_{k+1|k}\right] \tag{29}$$

Step 2.6: Estimate the Kalman gain

$$\boldsymbol{K}_{k+1} = \boldsymbol{P}_{k+1|k}^{XZ}(\boldsymbol{P}_{k+1|k}^{ZZ})^{-1} \tag{30}$$

Step 2.7: Estimate the updated state and the square-root factor of the corresponding error covariance matrix

$$\hat{\boldsymbol{X}}_{k+1|k+1} = \hat{\boldsymbol{X}}_{k+1|k} + \boldsymbol{K}_{k+1}(\boldsymbol{Z}_{k+1} - \hat{\boldsymbol{Z}}_{k+1|k}) \tag{31}$$

$$\boldsymbol{S}_{k+1|k+1} = \mathrm{Tria}([\boldsymbol{X}_{k+1|k} - \boldsymbol{K}_{k+1}\boldsymbol{Z}_{k+1|k}, \boldsymbol{K}_{k+1}\mathrm{Chol}(\boldsymbol{R}_{k+1})]) \tag{32}$$

B. RELOCATION AND NOVEL FORMULA FOR THE FADING FACTOR

The strong tracking filter (STF) utilizes the idea of fading memory by introducing the fading factor on the state prediction error covariance matrix in order to achieve the readjustment of gain matrix and to remain the orthogonality of residual error sequences. Therefore, the precision of the STF can be maintained when faced with the aircraft maneuvering. Reference [28] modified the calculation method of the fading factor through its equivalent expression and made it more applicable. Reference [19]–[25] apply the modified fading factor to nonlinear filters and structure multiple ST-nonlinear filters. However, as stated in Introduction, the two problems of the fading factor in [19]–[25] should be highlighted: the effective position and their form. Therefore, the effective position is relocated from the orthogonality principle and a novel calculation method is put forward: calculating the ratio between the identification value and the theoretical value in different dimensions respectively, and then select the maximum ratio as the fading factor. As such, the fading factor will remain the same sensitivity to the distance, the velocity and the angle dimension.

1) STF

The gain matrix can be adjusted in the STF to satisfy the following two equations.

$$E[(\boldsymbol{X}_{k+1} - \hat{\boldsymbol{X}}_{k+1|k})(\boldsymbol{X}_{k+1} - \hat{\boldsymbol{X}}_{k+1|k})^T] = \min \tag{33}$$

$$E[(\boldsymbol{Z}_{k+1+j} - \hat{\boldsymbol{Z}}_{k+1+j|k+j})(\boldsymbol{Z}_{k+1} - \hat{\boldsymbol{Z}}_{k+1|k})^T] = E[\boldsymbol{\nu}_{k+1+j}(\boldsymbol{\nu}_{k+1})^T] = \boldsymbol{0}, \quad k = 0, 1, 2\ldots;\ j = 1, 2, \ldots \tag{34}$$

where min means the estimation should achieve the least mean-square error. ν_{k+1} is the residual error in time $(k+1)T$. Eq. (34) reveals that the residual error sequences in different times should be orthometric. The steps of the STF can be summarized as:

$$\begin{aligned} \hat{\boldsymbol{X}}_{k+1|k} &= f(\hat{\boldsymbol{X}}_k) \\ \boldsymbol{P}_{k+1|k} &= \boldsymbol{\lambda}_{k+1}\boldsymbol{F}_{k+1|k}\boldsymbol{P}_k(\boldsymbol{F}_{k+1|k})^T + \boldsymbol{Q}_k \\ \hat{\boldsymbol{Z}}_{k+1|k} &= h(\hat{\boldsymbol{X}}_{k+1|k}) \\ \hat{\boldsymbol{X}}_{k+1} &= \hat{\boldsymbol{X}}_{k+1|k} + \boldsymbol{K}_{k+1}(\boldsymbol{Z}_{k+1} - \hat{\boldsymbol{Z}}_{k+1|k}) \\ \boldsymbol{K}_{k+1} &= \boldsymbol{P}_{k+1|k}(\boldsymbol{H}_{k+1})^T[\boldsymbol{H}_{k+1}\boldsymbol{P}_{k+1|k}(\boldsymbol{H}_{k+1})^T + \boldsymbol{R}_{k+1}]^{-1} \\ \boldsymbol{P}_{k+1} &= (\boldsymbol{I} - \boldsymbol{K}_{k+1}\boldsymbol{H}_{k+1})\boldsymbol{P}_{k+1|k} \end{aligned} \tag{35}$$

In application, the suboptimal calculation method is usually exploited for the fading factor λ_{k+1} [28].

2) MODIFIED FADING FACTOR

Before introducing the modified fading factor, *Theorem 1* is given as follows.

Theorem 1: The STF can't meet Eq. (33) and Eq. (34) simultaneously if the fading factor is introduced on the state prediction error covariance matrix.

As such, the introduced position should be relocated under the SCKF condition.

For Eq. (1) and Eq. (2), expand $\boldsymbol{Z}_{k+1}$ and $\boldsymbol{X}_{k+1}$ around $\boldsymbol{X}_k$ and $\hat{\boldsymbol{X}}_{k+1|k}$ and neglect its Taylor's series over two orders:

$$\boldsymbol{X}_{k+1} \approx f(\hat{\boldsymbol{X}}_k) + \boldsymbol{F}_{k+1|k}(\boldsymbol{X}_k - \hat{\boldsymbol{X}}_k) + \boldsymbol{W}_k \tag{36}$$

$$\boldsymbol{Z}_{k+1} \approx h(\hat{\boldsymbol{X}}_{k+1|k}) + \boldsymbol{H}_{k+1}(\boldsymbol{X}_{k+1} - \hat{\boldsymbol{X}}_{k+1|k}) + \boldsymbol{V}_{k+1} \tag{37}$$

where $\boldsymbol{H}_{k+1} = \left.\frac{\partial h}{\partial \boldsymbol{X}_{k+1}}\right|_{\boldsymbol{X}_{k+1}=\hat{\boldsymbol{X}}_{k+1|k}}$, $\boldsymbol{F}_{k+1|k} = \left.\frac{\partial f}{\partial \boldsymbol{X}_k}\right|_{\boldsymbol{X}_k=\hat{\boldsymbol{X}}_k}$. Additionally, Eq. (34) satisfies *theorem 2* [20], [29]:

Theorem 2: Assume that $\varepsilon_k = \boldsymbol{X}_k - \hat{\boldsymbol{X}}_k$, where $\hat{\boldsymbol{X}}_k$ is the state prediction value, if $O(|\varepsilon_k|^2) \ll O(|\varepsilon_k|)$, the covariance of residual error sequences in different times is

$$\begin{aligned} &E[\boldsymbol{v}_{k+1+j}(\boldsymbol{v}_{k+1})^T] \\ &= \boldsymbol{H}_{k+1+j}\boldsymbol{F}_{k+j}(\boldsymbol{F}_{k+j-1} - \boldsymbol{K}_{k+j}\boldsymbol{H}_{k+j}\boldsymbol{F}_{k+j-1})\cdots \\ &\quad (\boldsymbol{F}_{k+1} - \boldsymbol{K}_{k+2}\boldsymbol{H}_{k+2}\boldsymbol{F}_{k+1}) \\ &\quad \times E\left\{\boldsymbol{P}_{k+1|k}(\boldsymbol{H}_{k+1})^T - \boldsymbol{K}_{k+1}E[\boldsymbol{v}_{k+1}(\boldsymbol{v}_{k+1})^T]\right\} \end{aligned} \tag{38}$$

The equivalent formulation is

$$\boldsymbol{P}_{k+1|k}(\boldsymbol{H}_{k+1})^T - \boldsymbol{K}_{k+1}E[\boldsymbol{v}_{k+1}(\boldsymbol{v}_{k+1})^T] = \boldsymbol{0} \tag{39}$$

Assume that $\boldsymbol{P}^{XZ}_{k+1|k}$ is cross-covariance matrix between the state prediction error and the residual error before introducing the fading factor,

$$\boldsymbol{P}^{XZ}_{k+1|k} = E[(\boldsymbol{X}_{k+1} - \hat{\boldsymbol{X}}_{k+1|k})(\boldsymbol{Z}_{k+1} - \hat{\boldsymbol{Z}}_{k+1|k})^T] \tag{40}$$

Due to $\hat{\boldsymbol{X}}_{k+1} - \hat{\boldsymbol{X}}_{k+1|k}$ and $\boldsymbol{V}_{k+1}$ are mutually independent, substitute Eq. (37) into Eq. (40):

$$\begin{aligned} &\boldsymbol{P}^{XZ}_{k+1|k} \\ &= E[(\boldsymbol{X}_{k+1} - \hat{\boldsymbol{X}}_{k+1|k})(\boldsymbol{Z}_{k+1} - \hat{\boldsymbol{Z}}_{k+1|k})^T] \\ &= E\left\{(\boldsymbol{X}_{k+1} - \hat{\boldsymbol{X}}_{k+1|k})[\boldsymbol{H}_{k+1}(\boldsymbol{X}_{k+1} - \hat{\boldsymbol{X}}_{k+1|k}) + \boldsymbol{V}_{k+1}]^T\right\} \\ &= E[(\boldsymbol{X}_{k+1} - \hat{\boldsymbol{X}}_{k+1|k})(\boldsymbol{X}_{k+1} - \hat{\boldsymbol{X}}_{k+1|k})^T](\boldsymbol{H}_{k+1})^T \\ &= \boldsymbol{P}_{k+1|k}(\boldsymbol{H}_{k+1})^T \end{aligned} \tag{41}$$

Therefore, Eq. (39) is equal to

$$\boldsymbol{P}^{XZ}_{k+1|k} - \boldsymbol{K}_{k+1}E[\boldsymbol{v}_{k+1}(\boldsymbol{v}_{k+1})^T] = \boldsymbol{0} \tag{42}$$

$$\boldsymbol{K}_{k+1}(\boldsymbol{P}^{ZZ}_{k+1|k} - E[\boldsymbol{v}_{k+1}(\boldsymbol{v}_{k+1})^T]) = \boldsymbol{0} \tag{43}$$

Note that $\boldsymbol{K}_{k+1} \neq \boldsymbol{0}$. Therefore, the sufficient condition of the orthogonality is

$$\boldsymbol{P}^{ZZ}_{k+1|k} - E[\boldsymbol{v}_{k+1}(\boldsymbol{v}_{k+1})^T] = \boldsymbol{0} \tag{44}$$

Above all, the fading factor is introduced on the position of $\boldsymbol{P}^{ZZ}_{k+1|k}$ and $\boldsymbol{P}^{XZ}_{k+1|k}$. The residual error covariance matrix and the cross-covariance matrix in **Step 2.4** and **Step 2.5** in Section IV A should be recalculated as follows.

$$\boldsymbol{P}^{ZZ(\lambda)}_{k+1|k} = \boldsymbol{\lambda}_{k+1}(\boldsymbol{P}^{ZZ}_{k+1|k} - \boldsymbol{R}_{k+1}) + \boldsymbol{R}_{k+1} \tag{45}$$

$$\boldsymbol{P}^{XZ(\lambda)}_{k+1|k} = \boldsymbol{P}^{XZ}_{k+1|k}\boldsymbol{\lambda}_{k+1} \tag{46}$$

After introducing the fading factor, $\boldsymbol{K}_{k+1}$, $\hat{\boldsymbol{X}}_{k+1|k+1}$ and $\boldsymbol{S}_{k+1|k+1}$ also need to be recomputed. The other steps are the same as Section IV A.

Substitute Eq. (45) into Eq. (44),

$$E[\boldsymbol{v}_{k+1}(\boldsymbol{v}_{k+1})^T] - \boldsymbol{R}_{k+1} = \boldsymbol{\lambda}_{k+1}(\boldsymbol{P}^{ZZ}_{k+1|k} - \boldsymbol{R}_{k+1}) \tag{47}$$

$$E[\boldsymbol{v}_{k+1}(\boldsymbol{v}_{k+1})^T] = \begin{cases} \boldsymbol{v}_1(\boldsymbol{v}_1)^T & k=0 \\ \dfrac{\rho E[\boldsymbol{v}_k(\boldsymbol{v}_k)^T] + \boldsymbol{v}_{k+1}(\boldsymbol{v}_{k+1})^T}{1+\rho} & k \geq 1 \end{cases} \tag{48}$$

where ρ is the forgetting factor, satisfying $0 < \rho \leq 1$. Due to the invalid problem of the traditional fading factor, it is modified as:

$$\lambda_{k+1} = \begin{cases} c_{k+1} & c_{k+1} > 1 \\ 1 & c_{k+1} \leq 1 \end{cases} \tag{49}$$

$$c_{k+1} = \max\left\{\frac{[\text{diag}(\boldsymbol{N}_{k+1})]_i}{[\text{diag}(\boldsymbol{M}_{k+1})]_i}\right\}, \quad i = 1, 2, \ldots, l \tag{50}$$

$$\boldsymbol{N}_{k+1} = E[\boldsymbol{v}_{k+1}(\boldsymbol{v}_{k+1})^T] - \boldsymbol{R}_{k+1} \tag{51}$$

$$\boldsymbol{M}_{k+1} = \boldsymbol{P}^{ZZ}_{k+1|k} - \boldsymbol{R}_{k+1} \tag{52}$$

where diag(.) is the vector structured by diagonal elements. $[.]_i$ is ith element in the vector [.]. l is the total number of measurement dimension. Eq. (50) indicates that the maximum ratio in different dimensions will be chosen as the fading factor, thereby, the fading factor remains the same sensitive to different dimensions.

The differences between the modified fading factor and traditional ones are summarized as follows. (1) Traditional fading factor is introduced on the state prediction error covariance matrix, which can't simultaneously meet the two sufficient conditions of STF. However, the effective position of the proposed fading factor is deduced from the orthogonality principle and satisfies Eq. (33) and Eq. (34) simultaneously. (2) The proposed fading factor can adaptively tune the gain matrix according to the residual error. As such, the good tracking performance can be provided when faced with the abrupt state change. (3) The calculation of the proposed fading factor is determined by the maximum ratio in different dimensions of measurement. Therefore, the same sensitivity on different dimensions can be maintained, and the invalid problem can be avoided.

V. SIMULATIONS AND RESULTS

The simulations are run on a single Intel (R) Core (TM) i7-4790CPU(3.6GHz) processor with 4 GB memory, Windows 7 OS, and MATLAB 2014a. Two scenarios of aircraft maneuvering are tested and the three following algorithms are utilized as the baseline to compare against the proposed algorithm. The first is the integration of the CS model with the multiple-fading-factor SCKF [24] (CS-MSCKF). The second is the combination of the modified CS model [6] and the SCKF-STF [25] (MCS-SCKF-STF). The third is the IMM-SCKF. In the CS-MSCKF, $a_{\max} = 100m/s^2$ and $a_{-\max} = -120m/s^2$. The initial maneuvering frequency $\alpha_0 = 0.06$ and the forgetting factor $\rho = 0.95$ in the CS-MSCKF, MCS-SCKF-STF and the proposed algorithm. CV-CA-Singer models are adopted in IMM-SCKF. The standard deviations of the process noise of the CV model and CA model are 0.1 and 1 respectively. In the Singer model, $\alpha = 0.06$, $a_{\max} = 100m/s^2$, $p_0 = 0.1$ and $p_m = 0.8$. The transition probability is $\pi_{ii} = 0.9$, $\pi_{ij} = 0.05$, $i, j = 1, 2, 3$, $i \neq j$. The statistically average results are obtained through 500 Monte Carlo simulations. The root-mean-square error (RMSE) in time kT and the mean error (ME) in the whole simulation time are utilized as evaluation metrics:

$$E_{\mathrm{RMSE},k} = \left\{ \frac{1}{M} \sum_{j=1}^{M} \left\| \boldsymbol{X}_{i,k} - \hat{\boldsymbol{X}}_{i,k}^{j} \right\|_2^2 \right\}^{1/2} \tag{53}$$

$$E_{\mathrm{ME}} = \frac{1}{N} \sum_{k=1}^{N} E_{\mathrm{RMSE},k} \tag{54}$$

where $\boldsymbol{X}_{i,k}$ and $\hat{\boldsymbol{X}}_{i,k}^{j}$ are the real value and the estimation value of ith component of state vector in time kT in jth simulation respectively. M is the total number of simulations, and N is the total steps of simulation.

In the simulation, the state vector is $\boldsymbol{X} = [x, \dot{x}, \ddot{x}, y, \dot{y}, \ddot{y}]^T$, the measurement vector is $\boldsymbol{Z} = [r, \dot{r}, \theta]^T + \boldsymbol{V}_k$. Where $r = \sqrt{x^2 + y^2}$, $\dot{r} = (\dot{x}x + \dot{y}y)/r$, $\theta = \arctan(y/x)$, $\boldsymbol{V}_k \sim N(0, \boldsymbol{R}_k)$, $\boldsymbol{R}_k = \mathrm{diag}[\sigma_r^2, \sigma_{\dot{r}}^2, \sigma_\theta^2]$, which is the measurement noise covariance. $\sigma_r = 100m$, $\sigma_{\dot{r}} = 10m/s$, $\sigma_\theta = 0.1$rad. The measurement position (radar's position) is located in the original point of the coordinate system, and the aircraft trajectory is located in the same plane with the radar. The sample time $T = 1s$.

A. SCENARIO 1: MANEUVERING IN STEP ACCELERATION

In this scenario, the aircraft acceleration changes as steps. Fig. 1 (a) ∼ Fig. 1 (c) show the real trajectory, real velocity and real acceleration respectively. Fig. 2 (a) ∼ Fig. 2 (c) show RMSEs on the position estimation, velocity estimation and acceleration estimation of the four algorithms respectively. Table 1 shows MEs and runtime of the four algorithms.

Fig. 2 (a) ∼ Fig. 2 (c) show that the tracking precision on position, velocity and acceleration of the proposed algorithm are better than the three other algorithms whenever the aircraft is in the highly maneuvering state or the weak maneuvering state. Especially in the step jump accelerating state and the decelerating state, the peak error and the convergence time of the proposed algorithm are much smaller than the three other algorithms. Note that during 42 ∼ 52 s and 102 ∼ 112 s, the aircraft highly maneuvers in the angle dimension and weakly maneuvers in the distance dimension. As such, the fading factors in the CS-MSCKF and the MCS-SCKF-STF are both invalid. However, the proposed algorithm maintains the same sensitivity on different dimensions by introducing the modified fading factor. As such, the good performance is well maintained.

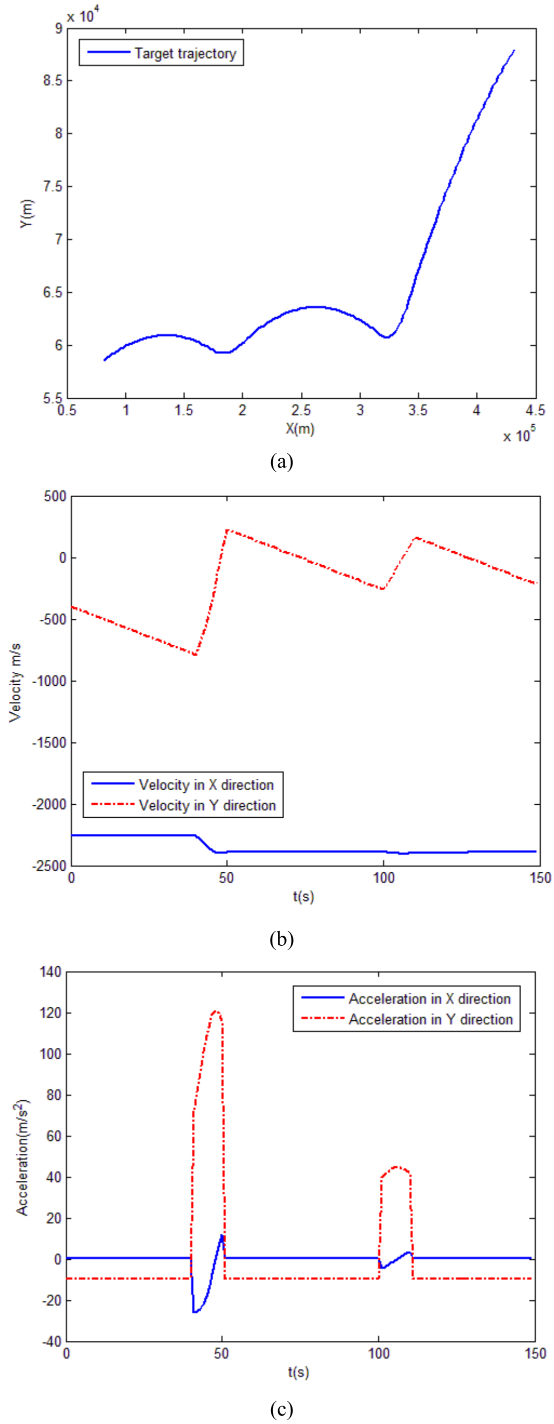

FIGURE 1. (a) Aircraft real trajectory. (b) Aircraft real velocity. (c) Aircraft real acceleration.

Table 1 depicts that the average tracking precision of the proposed algorithm is also better than the other three

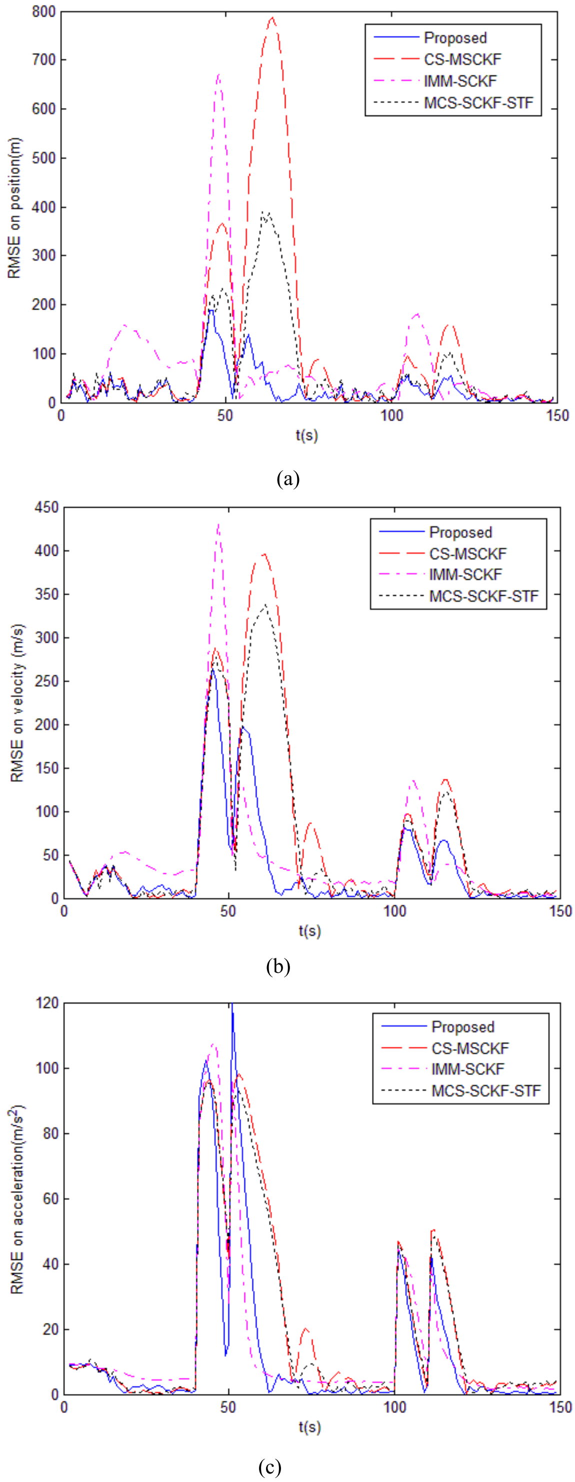

FIGURE 2. (a) Comparison of RMSEs on position estimation. (b) Comparison of RMSEs on velocity estimation. (c) Comparison of RMSEs on acceleration estimation.

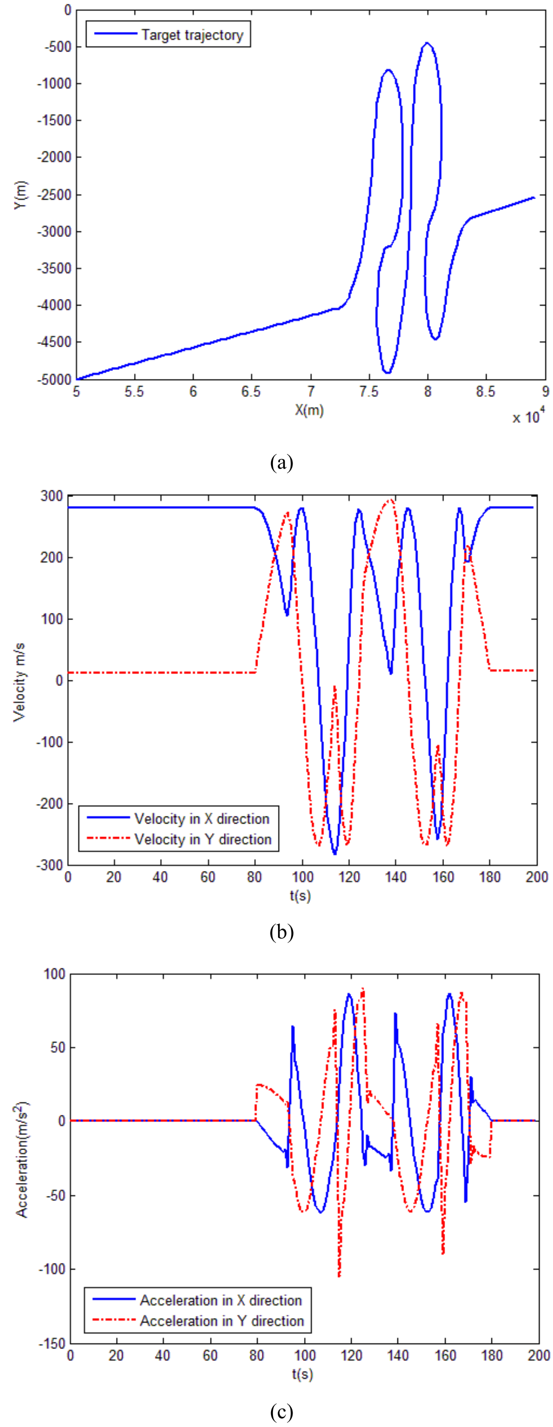

FIGURE 3. (a) Aircraft real trajectory. (b) Aircraft real velocity. (c) Aircraft real acceleration.

algorithms. MEs on the three dimensions are significantly decreased compare with the three other filters. Additionally, the proposed algorithm increases a little runtime compared with the two single-model filters. However, the much more performance improvement should be highlighted.

B. SCENARIO 2: HIGHLY MANEUVERING IN SNAKE SHAPES

In this scenario, the aircraft is firstly in the constant velocity, and then runs into highly maneuvering state, when accelerations in X coordinate and Y coordinate change drastically. Fig. 3(a) $\sim$ Fig. 3(c) show the aircraft real trajectory, real velocity and real acceleration respectively.

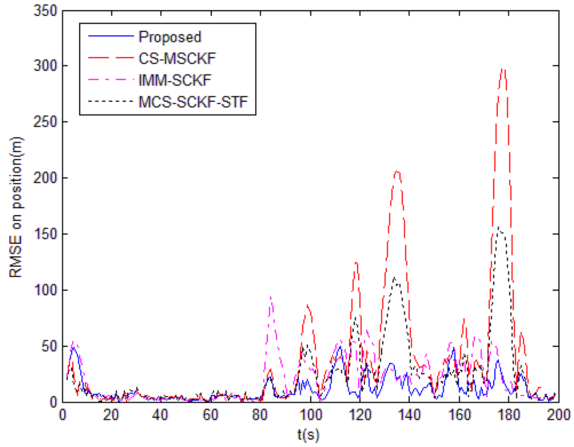

(a)

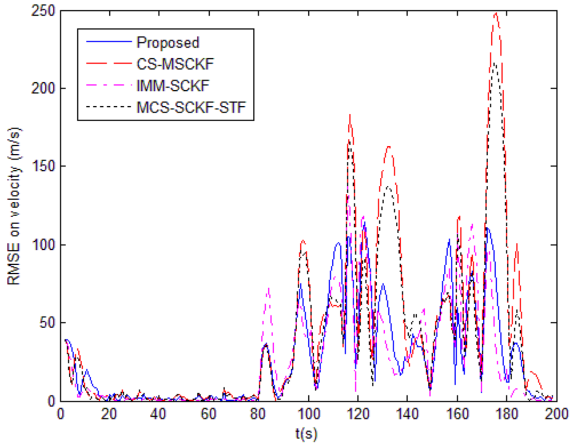

(b)

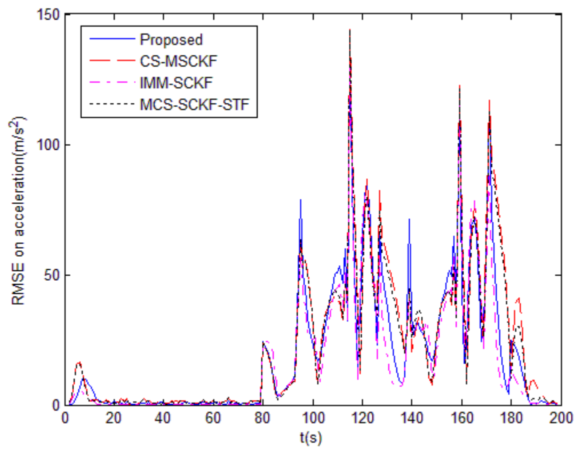

(c)

FIGURE 4. (a) Comparison of RMSEs on position estimation. (b) Comparison of RMSEs on velocity estimation. (c) Comparison of RMSEs on acceleration estimation.

Fig. 4(a) ∼ Fig. 4(c) show RMSEs on position estimation, velocity estimation and acceleration estimation of four algorithms respectively. Table 2 shows MEs and runtime of the four algorithms.

Fig. 4 (a) ∼ Fig. 4 (c) show that the tracking performance of the four algorithms approaches to each other when the aircraft is in the constant velocity state. However, when the aircraft is in the highly maneuvering state, RMSEs on the position and the velocity of the proposed algorithm is much lower than the other three algorithms. Though the peak of RMSE on the acceleration of the proposed algorithm is a little higher, it converges much quicker. Note that the maneuvering acceleration is within the preset $a_{\pm max}$ in the CS model, thus, the proposed adaptive CS model does perform better than the CS model. Additionally, during 80 ∼ 180 s, the aircraft continuously maneuvers in the distance and the angle dimension, leading to higher estimation errors of all algorithms. However, due to the modified fading factor, the same sensitivity on different dimensional maneuvering is maintained of the proposed algorithm. Furthermore, the adaptive adjustment of the CS model is realized and thus, the proposed algorithm achieves higher estimation precision.

Table 2 shows that MEs on the position, velocity and acceleration of the proposed algorithm are lower than the CS-MSCKF and the MCS-SCKF-STF. When compared with the IMM-SCKF, the proposed algorithm achieves better tracking performance on the position and approximate performance on the velocity and the acceleration. It is because the long time when the aircraft is in the constant velocity, with which the CV model in the IMM-SCKF can best matches. However, the proposed algorithm is modified from the CS model, which is originally designed for the maneuvering aircraft tracking. Thus, the tracking performance on the constant velocity of the proposed algorithm is a little worse than the IMM-SCKF, resulting in a little worse MEs on the velocity and the acceleration compared with the IMM-SCKF algorithm. However, the runtime of the proposed algorithm is much less than the later one.

C. ANALYSIS ON THE COMPUTATIONAL COMPLEXITY

Two dimensions of the state vector are added on the basis of the CS-MSCKF, thus, the computational complexity of the proposed algorithm increases around 1/3 compared with the former one. Though the state vector of the proposed algorithm also increases by two dimensions compared with the MCS-SCKF-STF, the calculation of the state noise covariance matrix is unnecessary and the fading factor calculation method in the MCS-SCKF-STF is more complex. Therefore, the computational complexity of the two algorithms is close. There is no need for the parameter calculation in the IMM-SCKF, but three models and SCK filters should work in parallel. Moreover, the input and the output interactive process are added. Therefore, the computational burden of the IMM-SCKF is 2.3 times of the CS-MSCKF [31] and thus 1.7 times of the proposed algorithm.

Above all, the proposed algorithm achieves better performance while maintaining a reasonably computational burden compared with the CS-MSCKF and the MCS-SCKF-STF. Additionally, the proposed algorithm obtains better performance on the continuous maneuvering by the more simple structure and less computational burden compared with the IMM-SCKF.

TABLE 1. Comparison of MES and runtime.

Algorithms	Mean error (ME)			Average runtime (s)
	Position (m)	Velocity (m/s)	Acceleration (m/s^2)	
Proposed	28.7077	35.1562	12.7666	0.0616
CS-MSCKF	113.7213	73.4408	20.1581	0.0447
IMM-SCKF	79.7119	49.9423	14.4312	0.1057
MCS-SCKF-STF	64.3337	64.5350	19.2406	0.0580

TABLE 2. Comparison of MES and runtime.

Algorithms	Mean error (ME)			average runtime (s)
	Position (m)	Velocity (m/s)	Acceleration (m/s^2)	
Proposed	11.4086	27.7363	20.1011	0.0827
CS-MSCKF	38.6490	43.1735	23.2248	0.0599
IMM-SCKF	19.6475	26.2997	17.6415	0.1401
MCS-SCKF-STF	23.8346	38.5114	22.3138	0.0781

VI. CONCLUSION

A novel strong tracking square-root cubature Kalman filtering algorithm based on the adaptive CS model is proposed aiming at the maneuvering aircraft tracking problem. The main work of this paper is summarized as follows.

(1) Two assumptions of the maximum acceleration and the mean acceleration in the CS model are combined with the MIE algorithm to introduce the Jerk input estimation and structure a modified CS model, which is connected with elements in the state estimation covariance matrix, thus, parameters in the proposed model can be adaptively adjusted.

(2) The introduced position of the fading factor is relocated from the orthogonality principle. Moreover, a new calculation method for the fading factor is proposed aiming at the problem of weak maneuvering on the distance and the velocity covering highly maneuvering on the angle in the existing fading factor.

(3) Simulation results of two maneuvering scenarios show that the proposed algorithm possesses better performance compared with the CS-MSCKF and the MCS-SCKF-STF. When compared with the IMM-SCKF, the proposed algorithm achieves better tracking performance on the position and the approximate tracking performance on the velocity and the acceleration while decreasing the runtime by 40%.

ACKNOWLEDGMENT

The authors are grateful to the Associate Editor and anonymous reviewers for their constructive comments and suggestions based on which this paper has been greatly improved.

REFERENCES

[1] R. A. Singer, "Estimating optimal tracking filter performance for manned maneuvering targets," *IEEE Trans. Aerosp. Electron. Syst.*, vol. AES-6, no. 4, pp. 473–4833, Jul. 1970.

[2] K. S. P. Kumar and H. Zhou, "A 'current' statistical model and adaptive algorithm for estimating maneuvering targets," *AIAA J. Guid.*, vol. 7, no. 5, pp. 596–602, 1984.

[3] K. Mehrotra and P. R. Mahapatra, "A Jerk model for tracking highly maneuvering targets," *IEEE Trans. Aerosp. Electron. Syst.*, vol. 3, no. 4, pp. 1094–1105, Oct. 1997.

[4] L. Chen, X. Gong, H. Shi, and J. Yang, "Maneuvering frequency adaptive algorithm of maneuvering target tracking," in *Proc. IEEE 4th Int. Conf. Intell. Control Inf. Process.*, Jun. 2013, pp. 455–458.

[5] D. Zhu, K. Chen, and W. Gen, "A new adaptive filtering algorithm based on the current statistical model," in *Proc. IEEE 5th Int. Conf. Intell. Hum.-Mach. Syst. Cybern.*, Aug. 2013, pp. 3–6.

[6] Y. Yang, X. Fan, S. Wang, Z. Zhuo, J. Nan, and L. Huang, "A new parameters adaptively adjusting method of current statistical model," in *Proc. IEEE Int. Conf. Inf. Autom.*, Aug. 2015, pp. 1738–1742.

[7] S. Julier, J. Uhlmann, and H. F. Durrant-Whyte, "A new method for the nonlinear transformation of means and covariances in filters and estimators," *IEEE Trans. Autom. Control*, vol. 45, no. 3, pp. 477–482, Mar. 2000.

[8] Y. Meng, S. Gao, Y. Zhong, G. Hu, and A. Subic, "Covariance matching based adaptive unscented Kalman filter for direct filtering in INS/GNSS integration," *Acta Astron.*, vol. 120, pp. 171–181, Mar. 2016.

[9] B. Jia, M. Xin, and Y. Cheng, "Sparse-grid quadrature nonlinear filtering," *Automatica*, vol. 48, no. 2, pp. 327–341, 2012.

[10] B. Jia, M. Xin, and Y. Cheng, "Sparse Gauss-ermite quadrature filter with application to spacecraft attitude estimation," *J. Guid. Control Dyn.*, vol. 34, no. 2, pp. 367–379, 2011.

[11] I. Arasaratnam and S. Haykin, "Cubature Kalman filters," *IEEE Trans. Autom. Control*, vol. 54, no. 6, pp. 1254–1269, Jun. 2009.

[12] I. Arasaratnam, S. Haykin, and R. T. Hurd, "Cubature Kalman filtering for continuous-discrete systems: Theory and simulations," *IEEE Trans. Signal Process.*, vol. 58, no. 10, pp. 4977–4993, Oct. 2010.

[13] Y. Huang and Y. Zhang, "Robust student's t-based stochastic cubature filter for nonlinear systems with heavy-tailed process and measurement noises," *IEEE Access*, vol. 5, pp. 7964–7974, 2017.

[14] A. H. Jazwinski, "Filtering for nonlinear dynamic systems," *IEEE Trans. Autom. Control*, vol. 11, no. 4, pp. 765–766, Oct. 1966.

[15] E. Villeneuve, W. Harwin, and W. Holderbaum, "Reconstruction of angular kinematics from wrist-worn inertial sensor data for smart home healthcare," *IEEE Access*, vol. 5, pp. 2351–2363, 2017.

[16] B. Cui, X. Chen, and X. Tang, "Improved cubature Kalman filter for GNSS/INS based on transformation of posterior sigma-points error," *IEEE Trans. Signal Process.*, vol. 65, no. 11, pp. 2975–2987, Jun. 2017.

[17] A. Sharma, S. C. Srivastava, and S. Chakrabarti, "A cubature Kalman filter based power system dynamic state estimator," *IEEE Trans. Instrum. Meas.*, vol. 66, no. 8, pp. 2036–2045, Aug. 2017.

[18] Y. Chen, Q. Zhao, Z. An, P. Lv, and L. Zhao, "Distributed multi-target tracking based on the K-MTSCF algorithm in camera networks," *IEEE Sensors J.*, vol. 16, no. 13, pp. 5481–5490, Jul. 2016.

[19] Z. Yin, G. Li, X. Sun, J. Liu, and Y. Zhong, "A speed estimation method for induction motors based on strong tracking extended Kalman filter," in *Proc. IEEE 8th Int. Power Electron. Motion Control Conf.*, May 2016, pp. 798–802.

[20] W. Huang, H. Xie, C. Shen, and J. Li, "A robust strong tracking cubature Kalman filter for spacecraft attitude estimation with quaternion constraint," *Acta Astron.*, vol. 121, pp. 153–163, Apr. 2016.

[21] D. Li, J. Ouyang, H. Li, and J. Wan, "State of charge estimation for $LiMn_2O_4$ power battery based on strong tracking sigma point Kalman filter," *J. Power Sources*, vol. 279, pp. 439–449, Apr. 2015.

[22] M. Narasimhappa, S. L. Sabat, and J. Nayak, "Adaptive sampling strong tracking scaled unscented Kalman filter for denoising the fibre optic gyroscope drift signal," *IET Sci., Meas. Technol.*, vol. 9, no. 3, pp. 241–249, Sep. 2015.

[23] A. Amirzadeh and A. Karimpour, "An interacting fuzzy-fading-memory-based augmented Kalman filtering method for maneuvering target tracking," *Digit. Signal Process.*, vol. 23, no. 5, pp. 1678–1685, Sep. 2013.

[24] N. Li, R. Zhu, and Y. Zhang, "A strong tracking square root CKF algorithm based on multiple fading factors for target tracking," in *Proc. IEEE 7th Int. Joint Conf. Comput. Sci. Optim.*, Jul. 2014, pp. 16–20.

[25] Q.-B. Ge, W.-B. Li, and C.-L. Wen, "SCKF-STF-CN: A universal nonlinear filter for maneuver target tracking," *J. Zhejiang Univ.-Sci. C (Comput. Electron.)*, vol. 12, no. 8, pp. 678–686, 2011.

[26] H. Khaloozadeh and A. Karsaz, "Modified input estimation technique for tracking manoeuvring targets," *IET Radar, Sonar Navigat.*, vol. 3, no. 1, pp. 30–41, 2009.

[27] X. R. Li and V. P. Jilkov, "Survey of maneuvering target tracking. Part I. Dynamic models," *IEEE Trans. Aerosp. Electron. Syst.*, vol. 39, no. 4, pp. 1333–1363, Oct. 2003.

[28] D. H. Zhou, Y. G. Xi, and Z. J. Zhang, "A suboptimal multiple fading extended Kalman filter," *Acta Automatica Sinica China*, vol. 17, no. 6, pp. 689–695, 1999.

[29] Z. Guo, L. J. Miao, and H. S. Zhao, "An improved strong tracking UKF algorithm and its application in SINS initial alignment under large azimuth misalignment angles," (in Chinese), *Acta Aeronautica Astron. Sinica*, vol. 35, no. 1, pp. 203–214, 2014.

[30] J. Fang, S. Dai, W. Xu, J. Zou, and Y. Wang, "Highly maneuvering hypervelocity-target tracking algorithm based on ST-SRCKF," (in Chinese), *J. Beijing Univ. Aeronautics Astron.*, vol. 42, no. 8, pp. 1698–1708, 2016.

[31] Z. Zhou, J. Liu, and X. Tan, "MCS model based on Jerk input estimation and nonlinear tracking algorithm," (in Chinese), *J. Beijing Univ. Aeronautics Astron.*, vol. 39, no. 10, pp. 1397–1402, 2013.

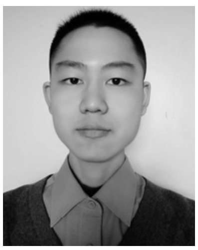

HAOWEI ZHANG received the bachelor's and master's degrees from the Air and Missile Defense College, Air Force Engineering University, Xi'an, China, in 2014 and 2016, respectively, where he is currently pursuing the Ph.D. degree. His research interests include multifunction radar resource management and intelligent scheduling.

JUNWEI XIE received the bachelor's, master's, and Ph.D. degrees from the Air and Missile Defense College, Air Force Engineering University, Xi'an, China, in 1993, 1996, and 2009, respectively. He is currently a Professor with the Air and Missile Defense College. His research interests include novel radar systems and jamming and anti-jamming.

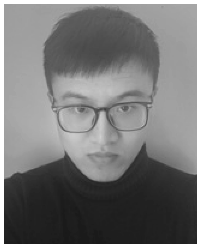

JIAANG GE received the bachelor's degree from the Beijing University of Aeronautics and Astronautics, Beijing, China, in 2017. He is currently pursuing the master's degree with the Air and Missile Defense College. His research interest is radar signal processing.

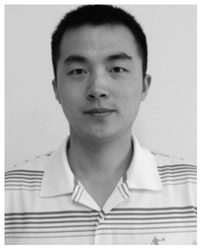

WENLONG LU received the bachelor's, master's, and Ph.D. degrees from the Air and Missile Defense College, Air Force Engineering University, Xi'an, China, in 2010, 2012, and 2016, respectively. He is currently an Engineer with Unit 94225, Chinese People's Liberation Army, Rizhao, China. His interests are time and frequency analysis.

BINFENG ZONG received the bachelor's, master's, and Ph.D. degrees from the Air and Missile Defense College, Air Force Engineering University, Xi'an, China, in 2010, 2012, and 2016, respectively. He is currently an Engineer with Unit 94710, Chinese People's Liberation Army, Wuxi, China. His interests include airborne electronic equipment and antenna array.